

Protoplanetary Disk Sizes and Angular Momentum Transport

Joan R. Najita

National Optical Astronomy Observatory, 950 N. Cherry Avenue, Tucson, AZ 85719

Edwin A. Bergin

Department of Astronomy, University of Michigan, 1085 S. University Avenue, Ann Arbor, MI 48109

ABSTRACT

In young circumstellar disks, accretion—the inspiral of disk material onto the central star—is important for both the buildup of stellar masses and the outcome of planet formation. Although the existence of accretion is well documented, understanding the angular momentum transport mechanism that enables disk accretion has proven to be an enduring challenge. The leading theory to date, the magnetorotational instability, which redistributes angular momentum within the disk, is increasingly questioned, and magnetothermal disk winds, which remove angular momentum from the disk, have emerged as an alternative theoretical solution. Here we investigate whether measurements of disk radii can provide useful insights into which, if either, of these mechanisms drive disk accretion, by searching for evidence of viscous spreading in gaseous disks, a potential signature of “in disk” angular momentum transport. We find that the large sizes of most Class II (T Tauri) gas disks compared to those of their earlier evolutionary counterparts, Class I gas disks, are consistent with expectations for viscous spreading in the Class II phase. There is, however, a large spread in the sizes of Class II gas disks at any age, including a population of very small Class II gas disks. Their small sizes may result from processes such as photoevaporation, disk winds, or truncation by orbiting low mass companions.

Subject headings: protoplanetary disks — accretion, accretion disks — stars: variables: T Tauri, Herbig Ae/Be

1. Introduction

Circumstellar disks play a starring role in the formation of stars and planets. Stars accrete a significant fraction of their mass through disks and planets form from the dust and

gas in disks. Disks surround all stars at birth because the material from which stars form, molecular cloud cores, possesses more angular momentum than can be contained in the star alone. As the disk evolves, the disk material spirals inward toward the star, is channeled onto stellar magnetic field lines, and eventually crashes onto the stellar surface, producing bright ultraviolet (UV) emission. From the luminosity of the UV excess, typical (few Myr old) T Tauri stars are inferred to accrete at a rate of $\sim 10^{-8} - 10^{-7} M_{\odot} \text{yr}^{-1}$ (Hartmann et al. 1998, 2016), and a $\sim 1 M_{\odot}$ star is inferred to grow in mass by a few percent to a few tens of percent during the T Tauri phase, the initial few Myr of its life.

Stellar accretion rates are well documented and characterized. With measurements now available for hundreds of young stars over a range of ages and masses, stellar accretion rates are found to decrease with stellar age (Sicilia-Aguilar et al. 2010; Manara et al. 2012; Antonucci et al. 2014; Venuti et al. 2014), increase with stellar mass (Muzerolle et al. 2003; Calvet 2004; Herczeg & Hillenbrand 2008; Fang et al. 2009; Alcalá et al. 2014; Antonucci et al. 2014; Manara et al. 2015; Natta et al. 2006), and are systematically reduced in transition objects, i.e., in disks with large central optically thin regions that may be forming giant planets (Kim et al. 2016; Najita et al. 2007, 2015).

The inspiral of the accreting disk gas is expected to affect the outcome of planet formation. Giant planets are expected to couple strongly to their gaseous disks and migrate inward from their formation distances along with the accretion of the disk toward the star. The resulting inward Type II migration is thought to explain the large number of giant exoplanets that are found much closer to their stars than Jupiter is in our solar system (e.g., Lin et al. 1996).

Despite the theoretical importance and documented existence of accretion, understanding exactly how disk accretion occurs, i.e., the mechanism that is responsible for disk angular momentum transport, has proven to be an enduring challenge. While the magnetorotational instability (MRI; Balbus & Hawley 1991) had been hailed as the answer to this question for a couple decades, recent work finds that non-ideal MHD effects suppress the instability in the planet formation region (1–10 AU), even in the upper disk layers, a consequence of the low ionization of T Tauri disks. With such “in disk” angular momentum transport thus apparently suppressed, magnetothermal disk winds launched from the disk surface have emerged as an alternative angular momentum removal mechanism (Bai & Stone 2013; Kunz & Lesur 2013; Gressel et al. 2015; Bai et al. 2016; see Turner et al. 2014 for a review).

Angular momentum transport occurs quite differently through disk winds and the MRI. The MRI redistributes angular momentum within the disk, so that a small fraction of the disk mass acquires most of the angular momentum, which allows the rest of the disk to accrete. The disk wind removes angular momentum from the disk in order to accomplish the

same objective. Neither mechanism has a verified observational signature thus far, making it difficult to determine which of these, if either, drive disk accretion.

Here we investigate whether measurements of disk radii can provide useful insights. If angular momentum transport within the disk is important, disks will spread with time as the fraction of the disk that takes up the excess angular momentum moves to larger radii and the remainder accretes (Lynden-Bell & Pringle 1974; Hartmann et al. 1998). If disk winds remove the excess angular momentum, disks need not grow in size with time.

Previous commentary on this topic has largely focused on the possible change in size with age of the *dust* component of Class II disks. In star-forming regions separated by a few Myr in age, the dust component of disks, as measured from submillimeter continuum emission, is found to be slightly larger for older disks in Lupus than those associated with the younger Taurus and Ophiuchus populations (Tazzari et al. 2017). While one might hope to detect more obvious evolution in disk size by comparing disk size measurements at 1–3 Myr to those of even older populations (~ 10 Myr), disk photoevaporation induced by stellar FUV irradiation has been argued to significantly reduce the size of a gaseous disk on few Myr timescales (e.g., Gorti et al. 2015). Photoevaporation will also strip away small grains that are coupled to the gas, potentially making the effect of viscous spreading difficult to detect at late times. Moreover, the likelihood that the large grains responsible for disk submillimeter emission migrate inward early in the evolution of disks (Takeuchi & Lin 2002, 2005; Birnstiel & Andrews 2014) suggests that submillimeter continuum measurements will underestimate the radii of Class II gas disks (e.g., Ansdell et al. 2018).

To sidestep these difficulties, here we compare the evolution in the size of *gaseous* disks, focusing on the evolution at earlier times, between the Class I and Class II phases. Section 2 describes the observational data that we use to address this issue. Sections 3 and 4 describe our result and its implications.

2. Methods and Data

To place an observational constraint on the mechanism that transports angular momentum in the T Tauri phase, we focus on the disk radii of Class I and Class II sources. Class I sources are young stellar objects that are still embedded in their molecular envelope. Stars accrete much of their mass during the Class I phase. Fed by infall from the molecular envelope, their surrounding disks are expected to be massive, with disk accretion likely to be driven by gravitational instability and possibly episodic in nature (Hartmann et al. 2016; Zhu et al. 2010). Class II sources are evolutionarily older: their infall having ceased and

their molecular envelopes dissipated, their disk mass declines with time as the star accretes through the disk at a more leisurely pace.

If the sizes of Class I disks establish the “initial” disk sizes at the beginning of the Class II phase, we can infer whether disks spread or not in the Class II phase as a consequence of accretion by comparing the sizes of Class I and Class II disks. The sizes of Class I disks will be affected by several factors: the angular momentum of the cloud core from which it formed, any magnetic braking that occurs in the collapse and infall process, as well as any spreading that occurs through disk angular momentum transport in the Class I phase. The sizes of Class II disks can also increase through viscous spreading as well as decrease through the action of FUV-driven photoevaporation and truncation by orbiting companions.

In measuring the size of a rotationally-supported disk in a Class I source, it is important to distinguish the disk emission from that of the infalling envelope. In contrast to a rotationally-supported disk, which will show a velocity trend of $v_\phi(r) \propto r^{-1/2}$ for Keplerian rotation, infalling gas at larger radii that conserves angular momentum will follow $v_\phi(r) \propto r^{-1}$. Harsono et al. (2013) argued that Class I disk sizes could be determined by searching for the radius where the velocity field transitions from $v_\phi \propto r^{-1}$ to $v_\phi \propto r^{-1/2}$. High angular resolution is needed to resolve the velocity field into these components.

Table 1 lists the properties of Class I sources with reported disk sizes that are derived in the above way from spatially resolved emission. The molecular tracers used are primarily CO and its isotopes, as well as HCO⁺ and CS. Because of the small number of Class I sources studied to date, we have also included Class 0 sources that have accretion rates and stellar masses similar to those of the Class I sources in Table 1. The stellar masses listed for these sources (referred to hereafter generically as “Class I sources”) are derived dynamically from the spatially resolved velocity structure of the disk.

To select Class I sources that are the plausible precursors of Class II T Tauri stars, we selected sources with stellar masses in the same range as the Class II sources ($0.3\text{--}1.3M_\odot$; see below). While the stellar masses of Class I sources will grow through accretion before reaching the Class II stage, including Class I sources in the same mass range as the Class II sources allows for the possibility that these sources are at the end of the Class I phase. This is a conservative choice in that more massive protostars tend to have larger disks. Note that several sources in Table 1 may evolve into Class II sources with stellar masses above $1.3M_\odot$ if they continue to accrete at their current rates for $\gtrsim 0.2$ Myr (e.g., L1551 IRS5; HH 212).

Because the sample size is small, IRS 63 is included for completeness, despite the fact that its near face-on geometry makes it difficult to distinguish between its disk and envelope (Brinch & Jorgensen 2013). Two sources that are well-known protostellar binaries (L1551

NE and L1551 IRS5) are also included for completeness, although their circumbinary disks may be preferentially larger than disks associated with single stars, e.g., if the system formed from high angular momentum material.

As shown in Table 1, the rotationally-supported disks of Class I sources with central stellar masses $< 1.0M_{\odot}$ have disk radii R_d from 50 AU to 300 AU with a typical value of ~ 100 AU.

To measure the size of Class II disks, we also use tracers of the gaseous component of disks rather than the dust. Disk solids are expected to experience significant inward radial drift relative to the gas (e.g., Takeuchi & Lin 2002, 2005; Brauer et al. 2008; Birnstiel & Andrews 2014). As a result, the size of the dust continuum emission underestimates the true disk size (e.g., Andrews et al. 2012; Huang et al. 2018; Liu et al. 2017; Ansdell et al. 2018) and gaseous tracers are preferred.

Good tracers of the radial extent of the gaseous disk would separate the disk emission from that of any surrounding molecular cloud. While estimates of disk radii made from CO emission work well in the absence of a surrounding molecular cloud, CN $N=2-1$ can be a better choice when a cloud is present. In their study of disks in the Taurus star forming region, Guilloteau et al. (2013; hereafter G13) showed that the CN $N=2-1$ emission from disks experiences little cloud contamination, is strong enough to be commonly detected, and is well-behaved.

Here we focus on gas disk sizes measured for Taurus because it is a relatively young star forming region (1–2 Myr), is well studied, and has limited contamination from the molecular cloud. We collated from the literature gas disk sizes for Class II sources with consistently determined mass and age estimates (Andrews et al. 2013), excluding sources with a spatially resolved stellar companion within $2''$. Stellar companions with a separation comparable to the disk size can truncate the outer radius of the disk (e.g., Artymowicz & Lubow 1994). As a result, sources such as RW Aur ($1.4''$), UY Aur ($0.88''$), T Tau ($0.7''$) are excluded. Because companions on scales much smaller than the disk ($\ll 1''$; e.g., GG Tau, DQ Tau) would not truncate the outer disk radius, systems with such companions are included.

As part of a study that used the Keplerian rotation signature of the CN $N=2-1$ emission from disks to derive stellar masses, Guilloteau et al. (2014; hereafter G14) reported gas disk outer radii determined from a power law fit to the emission that extends to an outer radius R_{out} , as derived from the IRAM interferometric data. The reported gas disk outer radii range from 225–750 AU. Guilloteau et al. (2016; hereafter G16) collated these and other gas disk sizes reported in the literature for Taurus sources, as measured interferometrically using the tracers CO, ^{13}CO , CN, and HCO^+ . Most of the interferometric radii in Table 2

(R_g , column 7) are from this compilation, supplemented by measurements from Simon et al. (2017). The errors on gas disk size reported in the literature range from 1% to 33% with a median error of 7% for the sources included in our study.

When spatially resolved data are unavailable, line fluxes F can be used instead to estimate the radial extent of the disk gas R_{out} when the system inclination is known. As described by G13, R_{out} can be derived using the relation $F = B_\nu(T)(\rho\Delta V)\pi R_{\text{out}}^2/D^2 \cos(i)$, where T is the average disk temperature, ΔV is the local line width, D is the distance, and ρ is a dimensionless parameter that depends on the line opacity. Disk sizes have been measured with this approach using CN $N=2-1$ emission (G13) and HCO⁺ $J=3-2$ emission (G16) assuming $\Delta V = 0.2 \text{ km s}^{-1}$ and $T=15 \text{ K}$. The line flux-based CN radii in Table 2 (R_{CN} , column 6) are from G13. As discussed by G16, the derived outer radii are very similar to (within 20% of) sizes obtained from resolved images made with interferometers, where available (see also Table 2).

As interferometric disk radii are available for most of the sources in Table 2, in our study we adopt these in lieu of the line flux-based sizes when available. The line flux-based CN radii are adopted for 6 sources, 4 of which are upper limits (DO Tau, FT Tau; upper limits for BP Tau, CIDA-11, DQ Tau, DR Tau).

For comparison with the radial extent of the gaseous emission, Table 2 also collates from the literature dust disk sizes, where available. Most of the values are from the study of Tripathi et al. (2017), who report dust disk sizes measured interferometrically from data obtained with the Submillimeter Array (SMA). Andrews & Williams (2007) report outer radii for the dust continuum emission for Taurus T Tauri stars. Other continuum sizes have been reported by Pietu et al. (2014) and Harris et al. (2012).

The outer dust disk radii reported by Pietu et al. (2014), based on data from the IRAM Plateau de Bure interferometer, come from fitting the visibilities to a parametric model that assumes a power law surface density distribution $\Sigma(r) \propto r^{-p}$ for disk radii r out to an outer radius R_{out} and a power law index $p = 1$. As they note, the derived size is relatively insensitive to the choice of p . Disk radii would be $\sim 15\%$ smaller for $p = 0$ and $\sim 5\%$ larger for $p = 2$. The outer disk radii reported by Harris et al. (2012), based on data taken with the Submillimeter Array (SMA), were similarly obtained by fitting the disk emission to a simple parametric model with surface brightness $I_\nu \propto r^{-1.5}$ out to an outer radius R_d . They estimate that altering the power law index by $\pm 30\%$ would change the disk size by $\sim 20\%$ to 40% , with steeper (shallower) gradients corresponding to larger (smaller) disk sizes.

Tripathi et al. (2017) model the SMA visibility data using a more complex 5-parameter “Nuker” profile for the intensity, $I_\nu(r) \propto (r/t_t)^{-\gamma}[1 + (r/r_t)^\alpha]^{(\gamma-\beta)/\alpha}$, that is capable of fitting

the wide range of morphologies of disks, from continuous disks to the ring-like emission of transition objects. From the fits, one can retrieve the emission size of the disk R_{eff} that encompasses a fixed fraction of the total flux. Although Tripathi et al. (2017) tabulate disk sizes that enclose 68% of the total flux, here we use the corresponding values that enclose 90% of the total flux, which more closely captures the radial extent of the disk continuum emission.

The errors on dust disk size reported by Tripathi et al. are 1% to 13% with a median of 5% for the sources included here. Pietu et al. (2017) reported larger errors (5% to 27%) on dust disk size, with a median of 11% for the sources included in our study.

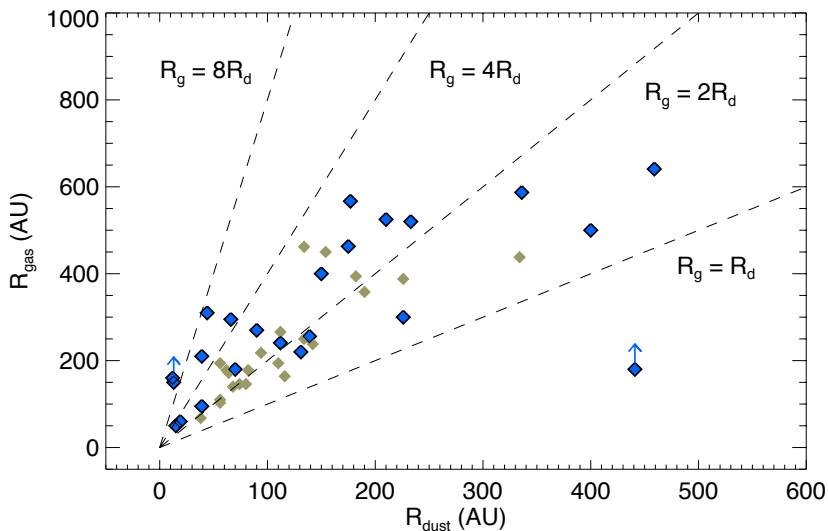


Fig. 1.— Sizes of Class II disks in Taurus (large blue diamonds) as measured interferometrically from dust continuum emission and gaseous tracers, for all sources where both measurements are available. Sources have gas disks typically 1.5 to 8 times larger than their dust disks. Many gas disks are larger than 200 AU. Similar results reported by Ansdell et al. (2018) are also shown (small gray diamonds).

3. Results

Figure 1 compares the millimeter continuum sizes of dust disks and gaseous disks, both measured interferometrically, for sources where both measurements are available. As found in other studies of individual sources (e.g., Andrews et al. 2012; Huang et al. 2018; Liu et al. 2017; see also Isella et al. 2007; Panic et al. 2009; de Gregorio-Monsalvo et al. 2013;

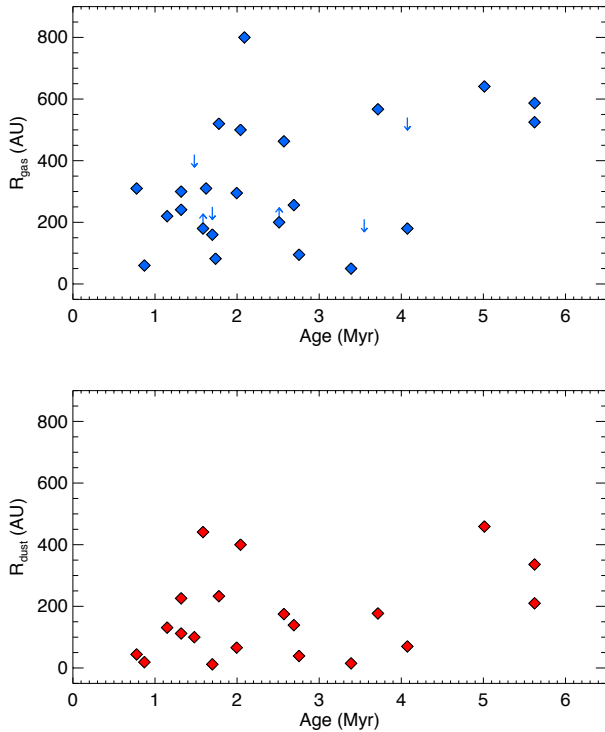


Fig. 2.— Sizes of gas dust disks of Taurus classical T Tauri stars as a function of stellar age. Gas disk sizes (top) are measured from interferometrically for the vast majority of sources (blue diamonds) or have an upper limits from CN line fluxes (blue downward arrows). Dust disk sizes (bottom) are measured interferometrically from submillimeter continuum emission.

Cleeves et al. 2016) and star formation regions (Ansdell et al. 2018), the gaseous component of disks extends to larger radii than the dust component. In this sample, sources have gas disks typically 1.5 to 8 times larger than their dust disks, with most gas disks larger than 200 AU. The larger sizes of Class II gas disks compared to Class II dust disks are likely the result of inward radial drift of dust through aerodynamic drag.

Similar to the situation found here for the Taurus disks, Ansdell et al. (2018) reported that the gas disks of 22 sources in the Lupus star forming region are uniformly larger than their dust disks by a factor of 1.5 to 3. As they describe, the difference could be due to either the inward drift of disk solids relative to the gas and/or optically thick gas emission. In the latter scenario, the CO emission is optically thick, making it easier to detect at larger radii than optically thin dust continuum. Ansdell et al. (2018) found that while optical depth effects could account for the lower R_g/R_d values they observed, radial drift was needed to explain the higher observed values. In either case, the true radial extent of the disk is best

probed with a gaseous tracer.

Figure 2 plots the gas and dust disk sizes as a function of stellar age (Andrews et al. 2013, using the Siess et al. 2000 tracks) for all sources from Table 2 in a stellar mass range ($0.3\text{--}1.3 M_{\odot}$) appropriate for the evolutionary descendants of the Class I sources in Table 1. That is, we exclude both very low mass stars (CIDA-1, CIDA-8, FN Tau, FP Tau) as well as intermediate mass T Tauri stars and Herbig stars (AB Aur, CW Tau, MWC758, RY Tau, SU Aur, and T Tau). The gas disk sizes shown are measured interferometrically for the vast majority of sources (blue diamonds) or have an upper limit from their CN line flux (downward blue arrows; G13). There is a large range in disk size at any age and no strong trend of size with age, although sources with gas disks larger than 400 AU are older than 1.5 Myr.

The gaseous disk sizes in Figure 2 include measurements made with CN, which may underestimate the gas disk size. Because CN $N=2-1$ can be subthermally populated, it may not trace the full extent of the gas disk. Guilloteau et al. (2016) find that $\text{HCO}^+ J=3-2$, which is better thermalized than CN, is optically thick and a good measure of the extent of the gas disk. When both diagnostics are measured, the CN size is often smaller.

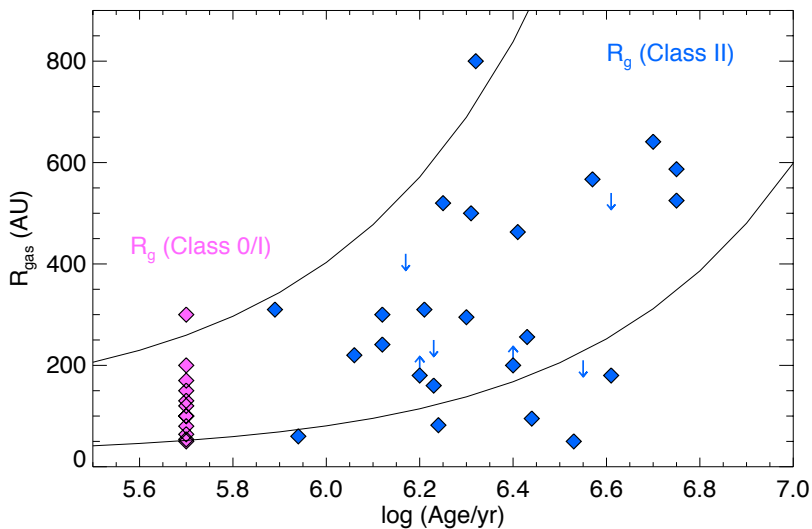


Fig. 3.— Observed gas disk radii of Class I disks (pink diamonds) and Taurus Class II disks (blue diamonds and arrows). The solid lines show the disk radii that contain 90% of the disk mass in simple models of viscously spreading disks (see text for details). Most of the Class II gas disk sizes fall between these two lines.

Figure 3 compares the gas disk sizes of Class II sources from Figure 2 (blue diamonds and arrows) with those of Class I sources (pink diamonds). The latter are placed at an

nominal age younger than 1 Myr. While almost all of the Class I gas disk radii are smaller than 200 AU, 2/3 of the Taurus Class II disk radii are larger than 200 AU. If Class I disks represent the initial conditions for the evolution of Class II disks, these two properties suggest that gas disks grow in size in the T Tauri phase.

The Class II disk sizes are roughly consistent with the sizes expected for sources that start out at the sizes of Class I disks and spread with time as they accrete. To illustrate this, we can consider the evolution of a T Tauri “ α -disk”. The observed evolution in stellar accretion rates with time can be explained as a consequence of disk evolution through a viscous process in which viscosity is parameterized as $\nu = \alpha c_s H$, where c_s is the sound speed, H the disk scale height, and $\alpha \simeq 0.01$ is the viscosity parameter (Hartmann et al. 1998; Sicilia-Aguilar et al. 2010).

As described by Hartmann et al. (1998), if the viscosity varies with disk radius R as a power law ($\nu \propto R^\gamma$), the viscous evolution of the disk has a similarity solution (Lynden-Bell & Pringle 1974), with $\gamma = 1$ corresponding to the usual assumption of a viscosity parameter α that is roughly constant with radius. In this case, the fraction of the disk mass interior to radius R at time t ,

$$\frac{M_d(R, t)}{M_d(t)} = 1 - \exp\left(-\frac{R}{R_1 T}\right),$$

where R_1 is the radius that initially contains ~ 0.6 of the total disk mass, T is the non-dimensional time $T = t/t_s + 1$. In this expression t_s is the viscous scaling time $t_s = R_1^2/3\nu_1$, where ν_1 is the viscosity at R_1 , so that

$$t_s \sim 0.08 \text{ Myr} \left(\frac{\alpha}{10^{-2}}\right)^{-1} \left(\frac{R_1}{10 \text{ AU}}\right) \left(\frac{M_*}{0.5}\right)^{1/2} \left(\frac{T_d}{10 \text{ K}}\right)^{-1},$$

where T_d is the disk temperature at 100 AU.

The solid lines in Figure 3 show, as a function of time, the disk radii that contain 90% of the disk mass, assuming a typical T Tauri stellar mass $M_* = 0.5M_\odot$ and a typical disk temperature of 10 K at 100 AU. The curves assume two different initial disk sizes and viscosities: $R_1 = 50$ AU and $\alpha = 0.01$ (upper line) and $R_1 = 10$ AU and $\alpha = 0.002$ (lower line). The range in R_1 is chosen to span the sizes of Class I disks. Most of the Class II disk sizes fall between these two lines.

To include the Lupus sources in the comparison of Class I and Class II disk sizes, we also show in Figure 4 the size distributions of Class II gas disks in Taurus (blue) and Lupus (gray) and Class I gas disks (pink), shown differentially and as a cumulative fraction (lower right). The cumulative size distribution of the combined (Taurus and Lupus) Class II gas disk samples is also shown (cyan; lower right). Like the Taurus sources, the Lupus sample

is restricted to the stellar mass range $0.3\text{--}1.3 M_{\odot}$ using the masses from Alcalá et al. (2014, 2017; see also online tables in Ansdell et al. 2018); sources with a known binary companion within $2''$ are also excluded (Sz 68 and Sz 123A; Ghez et al. 1997). For the Taurus sources with upper limits on disk mass (4 sources), the disk size is taken as 50% of the upper limit value. The results are not sensitive to the exact value. While only 23% of the Class I gas disks are larger than 200 AU, a much larger fraction of the Taurus (68%) and Lupus (50%) Class II gas disks are larger than 200 AU.

From the two-sample K-S test, we find that the probability is $< 1\%$ that the Taurus and Class I gas disk sizes are drawn from the same distribution. Similarly, the probability that the combined (Taurus and Lupus) Class II gas disk sizes are drawn from the same distribution as the Class I gas disk sizes is also $< 1\%$. Because the Class I sample is small, the results are sensitive to which sources are included in the comparison. If we exclude L1551 NE (a binary with large 300 AU gas disk) from the Class I sample, the probability that the Class II and Class I sizes are drawn from the same distribution drops to 0.2%.

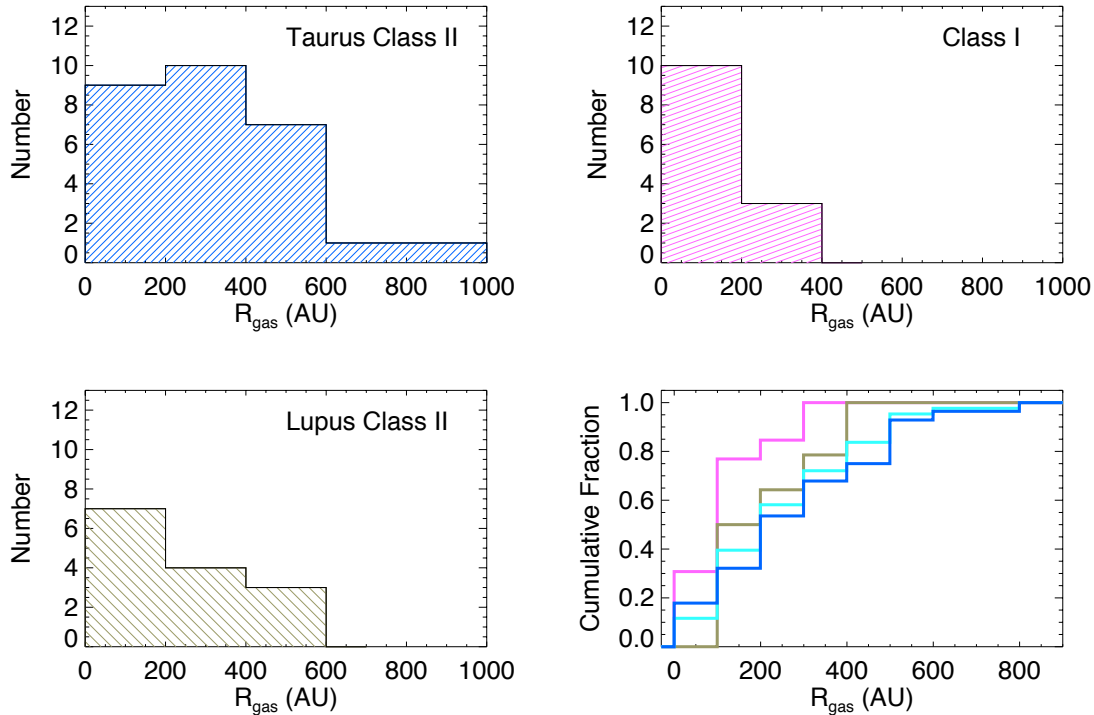


Fig. 4.— Gas disk sizes of Class II sources in Taurus (blue) and Lupus (gray) and Class I sources (pink) shown differentially and as a cumulative fraction (lower right). In the lower right panel, the cumulative distribution of the combined (Taurus and Lupus) Class II gas disks is also shown (cyan). Class I gas disks are smaller than Class II gas disks.

4. Discussion

As shown in the previous section, most Class II disks in Taurus are larger in radius than the Class I disks that have been studied to date, consistent with expectations for disk spreading, i.e., angular momentum transport within the disk in the Class II phase. Disks might spread as a consequence of angular momentum transport through gravitational instability (e.g., review by Kratter & Lodato 2016) or viscous transport (e.g., review by Hartmann et al. 2016). Processes other than such “in-disk” angular momentum transport tend to reduce the sizes of gas disks. Photoevaporation by stellar FUV irradiation acts to truncate the disk at large radii and cause it to shrink with time, even in the presence of viscous spreading (Gorti et al. 2015). If magnetothermal winds (Bai & Stone 2013; Bai et al. 2016) remove angular momentum efficiently from disks, disks could accrete without needing to spread with time. The formation of giant planets at large radii can also truncate disks.

Our result complements observational and theoretical studies of angular momentum transport in disks. While the MRI (Balbus & Hawley 1991; Gammie 1996) has long been the favored mechanism for disk accretion in the T Tauri phase, recent theoretical studies that explore the impact of non-ideal MHD effects have seriously questioned whether the MRI can operate in T Tauri disks, especially at radii relevant to planet formation $\sim 1\text{--}10$ AU. Winds launched by a combination of magnetic and thermal effects have been proposed as an alternative transport mechanism (Bai & Stone 2013; Kunz & Lesur 2013; Simon et al. 2013a, 2013b, 2015; Lesur et al. 2014; Gressel et al. 2015; Bai et al. 2016; Bai & Stone 2017; see Turner et al. 2014 for a review).

Neither mechanism (MRI or magnetothermal winds) has a verified observational signature thus far at these distances. Disk turbulence possibly driven by the MRI has been detected both within 1 AU and beyond 40 AU. At disk radii within 0.3 AU, high resolution spectroscopy of CO overtone emission has uncovered evidence for non-thermal velocities comparable to the sound speed in the disk atmospheres of a few young stars (e.g., Carr et al. 2004; Najita et al. 1996; 2009; Doppmann et al. 2008), consistent with the non-thermal motions expected for MRI-driven turbulence. High resolution ALMA observations of outer disks appear to favor low levels of non-thermal broadening, at only $\sim 5\text{--}10\%$ of the sound speed (HD163296 and TW Hya–Flaherty et al. 2015, 2018; de Gregorio-Monsalvo et al. 2013). However, turbulence at a larger fraction of the sound speed ($\sim 20\%$) has recently been detected in the outer disk of DM Tau (K. Flaherty 2018, private communication). No signature of turbulence has yet been reported at the disk radii where non-ideal MHD effects are expected to strongly suppress the MRI (1–10 AU).

The existence and character of magnetothermal winds are also uncertain. Theoretical studies predict that winds capable of driving disk accretion at the observed stellar accre-

tion rates will be massive, with mass loss rates comparable to disk accretion rates. It has been suggested that the low velocity component of the OI 6300Å line emission from T Tauri stars provides evidence for magnetothermal winds (Simon et al. 2016). However, the decomposition of a complex OI 6300Å profile into multiple components potentially introduces uncertainty in the interpretation. More detailed studies of this and other diagnostics, combined with quantitative theoretical predictions of observable wind signatures can potentially verify the existence and angular momentum transport properties of magnetothermal winds.

In the meantime, the larger sizes of most Taurus Class II disks compared to Class I disks strongly suggest that angular momentum redistribution within the disk, by some mechanism, plays a large enough role in disk evolution that a large fraction of disks spread significantly from the Class I to Class II phases. The data do not comment on whether the mechanism responsible is the MRI or other processes. Disk winds may also remove angular momentum but not enough to prevent the spreading of these disks.

These results complement earlier commentary on the evolution of (primarily dust) disk sizes that found tentative, sometimes conflicting, results. Although Andrews et al. (2007) seemed to find no trend of dust disk size with age among Class II objects (their Fig. 15), subsequent studies found tentative evidence that dust disk sizes do increase with age (Isella et al. 2009, their Figure 10; Guilloteau et al. 2011, their Figure 13). More recently, Tazzari et al. (2017) found that in star-forming regions separated by 1–2 Myr in age, the sizes of Class II disks, as measured from submillimeter *continuum* emission, are slightly larger for disks in Lupus (1–3 Myr) than those in the slightly younger Taurus and Ophiuchus (1–2 Myr) populations. They tentatively attributed the size difference to viscous evolution. Thus, the evidence for increasing *dust* disk size with age during the Class II phase is modest to uncertain, consistent with the picture from Figure 2.

Of the 22 Lupus Class II disks in the recent study by Ansdell et al. (2018), which range in size from ~ 100 AU to ~ 500 AU, approximately half have gas disk radii > 200 AU, a smaller fraction than in the Taurus sample studied here but still quite large. Although the authors did not compare the sizes of Class I gas disks with their Class II gas disk sizes, it seems clear that if the Class I disks from Table 1 are typical of the evolutionary precursors of the Lupus Class II disks, the large gas disks (> 200 AU) among the Lupus population also suggest that viscous spreading occurs in the T Tauri phase (Figure 4).

For the purpose of this study, the Lupus disks are less ideal than the Taurus disks for two reasons. Firstly, the binarity of sources in Lupus is not as completely characterized as that of Taurus sources. As a result, some Lupus disks may possess unknown stellar companions that have dynamically truncated their gaseous disks. Secondly, Lupus is an older star forming region (~ 3 Myr) than Taurus (1–2 Myr). As a result, photoevaporation has had more time

to evaporate away outer disks (Gorti et al. 2015). Giant planets, which have had more time to form in older systems, can also truncate disks dynamically. Despite these possible effects, the Lupus Class II disks still appear larger than the Class I disks.

More extensive measurements of gas disk sizes are needed to understand the timing and extent of “in-disk” angular momentum transport. Among the Class II disks studied here, there is a likely bias toward larger disks which are brighter and easier to study and resolve. Measurements of disk radii for a larger number of disks would illuminate the full range and frequency of gas disk sizes as a function of age. At the present time, the existence of a large number of disks that are larger than Class I gas sizes (Fig. 3) strongly suggests that at least some disks spread in the Class II phase.

One of the limitations of this study is the small number of Class I sources with reported gas disk radii. The presence of an infalling envelope also makes it challenging to measure Class I gas disk sizes; future work may find a way around this difficulty. If future studies of a larger population of Class I sources find disks systematically much larger than those studied to date, our conclusion will need to be revised. Further measurements of Class I disks can also reveal when disk spreading occurs. One might argue that the larger sizes of Class II disks are an outcome of viscous spreading in the Class I phase rather than the Class II phase. If true, surveys of a larger number of Class I disks should encounter Class I disks with larger sizes.

Interestingly there is, in addition to the majority of large disks (> 200 AU), a population of very small gas disks over a range of ages (< 100 AU). The small disks shown in Figure 3 come primarily from the sample studied by Simon et al. (2017). These authors suggested that the small gas disk sizes they measured were due in part to the cooler effective temperatures of the stars in their sample. However, we did not find a strong trend between stellar luminosity and gas disk size in the sample studied here. Such small disks are not anticipated at ages of several Myr if all disks spread with an effective viscosity of $\alpha > 0.001$. These systems may be disks that are truncated from the outside by photoevaporation, disk winds, or planetary companions. Further observations of these systems, to search for winds or companions, can test these ideas.

We thank the Kavli Institute for Theoretical Physics for their stimulating research environment and research support, which led us to pursue the ideas explored here. We also thank Megan Ansdell, Scott Kenyon, and the referee, Michal Simon, for helpful advice and careful readings of the manuscript. J. N. acknowledges the stimulating research environment supported by NASA Agreement No. NNX15AD94G to the “Earths in Other Solar Systems” program. This research was supported in part by the National Science Foundation under

Grant No. NSF PHY-1748958.

References

- Alcalá, J. M., Natta, A., Manara, C. F., et al. 2014, *AA*, 561, 2
- Alcalá, J. M., Manara, C. F., Natta, A. et al. 2017, *AA*, 600, 20
- Andrews, S. M., Wilner, D. J., Hughes, A. M., et al. 2012, *ApJ*, 744, 162
- Andrews, S. M., Rosenfeld, K. A., Kraus, A. L., & Wilner, D. J. 2013, *ApJ*, 771, 129
- Ansdell, M., Williams, J. P., Trapman, L., et al. 2018, *ApJ*, 859, 21
- Antonucci S., García López R., Nisini B., et al. 2014, *AA*, 572,62
- Artymowicz, P. & Lubow, S. H. 1994, *ApJ*, 421, 651
- Aso, Y., Ohashi, N., Saigo, K., et al. 2015, *ApJ*, 812, 27
- Bai, X. & Stone, J. M. 2013, *ApJ*, 769, 76
- Bai, X., Ye, J., Goodman, J., & Yuan, F. 2016, *ApJ*, 818, 152
- Bai, X., & Stone, J. M. 2017, *ApJ*, 843, 36
- Balbus, S. A., & Hawley, J. F. 1991, *ApJ*, 376, 214
- Birnstiel, T., & Andrews, S. M. 2014, *ApJ*, 780, 153
- Brauer, F., Dullemond, C. P., Henning, Th. 2008, *AA*, 480, 859
- Brinch, C., & Jorgensen, J. K. 2013, *AA*, 559, 82
- Calvet N. 2004, In “Stars as Suns: Activity, Evolution and Planets”, Proc. Symp. Int. Astron. Union, 219th, Sydney, July 21-25, 2003, ed. A. K. Dupree, A. O. Benz, (San Francisco: ASP), pp. 599-609.
- Carr, J. S., Tokunaga, A. T., & Najita, J. 2004, *ApJ*, 603, 213
- Chapillon, E., Guilloteau, S., Dutrey, A., & Piétu, V. 2008, *A&A*, 488, 565
- Chou, T.-L., Takakuwa, S., Yen, H.-W., Ohashi, N., & Ho, P. T. P. 2014, *ApJ*, 796, 70
- Cleeves, L. I., Öberg, K. I., Wilner, D. J., et al. 2016, *ApJ*, 832, 110
- Coffey, D., Dougados, C., Cabrit, S., Pety, J., & Bacciotti, F. 2015, *ApJ*, 804, 2
- de Gregorio-Monsalvo, I., Ménard, F., Dent, W., et al. 2013, *AA*, 557, A133
- Doppmann, G. W., Najita, J. R., & Carr, J. S. 2008, *ApJ*, 685, 298

- Dutrey, A., Guilloteau, S., Prato, L., et al. 1998, *A&A*, 338, L63
- Fang, M., van Boekel, R., Wang, W., et al. 2009, *AA*, 504, 461
- Flaherty, K. M., Hughes, A. M., Rosenfeld, K. A., et al. 2015, *ApJ*, 813, 99
- Flaherty, K. M., Hughes, A. M., Teague, R., et al. 2018, *ApJ*, 856, 117
- Gammie, C. F. 1996, *ApJ*, 457, 355
- Ghez, A. M., McCarthy, D. W., Patience, J. L., & Beck, T. L. 1997, *ApJ*, 481, 378
- Gorti, U., Hollenbach, D., & Dullemond, C. P. 2015, *ApJ*, 804, 29
- Gressel, O., Turner, N. J., Nelson, R. P. & McNally, C. P. 2015, *ApJ*, 801, 84
- Guilloteau, S., Dutrey, A., & Simon, M. 1999, *A&A*, 348, 570
- Guilloteau, S., Di Folco, E., Dutrey, A., et al. 2013, *AA*, 549, 92
- Guilloteau, S., Simon, M., Piétu, V., Di Folco, E., Dutrey, A., Prato, L., & Chapillon, E. 2014, *AA*, 567, 117
- Guilloteau, S., Reboussin, L., Dutrey, A., et al. 2016, *AA*, 592, 124
- Guilloteau, S., Dutrey, A., Piétu, V., & Boelher, Y. 2011, *AA*, 529, 105
- Harris, R. J., Andrews, S. M., Wilner, D. J., & Kraus, A. L. 2012, *ApJ*, 751, 115
- Harsono, D., Visser, R., Bruderer, S., van Dishoeck, E. F., & Kristensen, L. E. 2013, *AA*, 555, 45
- Harsono, D., Jörgensen, J. K., van Dishoeck, E. F., et al. 2014, *A&A*, 562, 77
- Hartmann, L., Calvet, N., Gullbring, E., & D'Alessio, P. 1998, *ApJ*, 495, 385
- Hartmann, L., Herczeg, G., & Calvet, N. 2016, *ARAA*, 54, 135
- Herczeg G. J., Hillenbrand, L. A. 2008, *ApJ*, 681, 594
- Huang, J., Andrews, S. M., Cleeves, L. I., et al. 2018, *ApJ*, 852, 122
- Isella, A., Testi, L., Natta, A., et al. 2007, *AA*, 469, 213
- Isella, A., Carpenter, J. M., & Sargent, A. I. 2009, *ApJ*, 701, 260
- Jensen, E. L. N., & Akeson, R. 2014, *Nature*, 511, 567
- Kessler-Silacci 2004, Ph.D. Thesis

- Kim, K. H., Watson, D. M., Manoj, P., et al. 2016, *ApJS*, 226, 8
- Kratter, K. & Lodato, G. 2016, *ARAA*, 54, 271
- Kunz, M. W. & Lesur, G. 2013, *MNRAS*, 434, 2295
- Lee, C.-F., Hirano, N., Zhang, Q., et al. 2014, *ApJ*, 786, 114
- Lesur, G., Kunz, M. W., & Fromang, S. 2014, *AA*, 566, 56
- Lin, D. N. C., Bodenheimer, P., & Richardson, D. C.
- Liu, Y., Henning, Th., Carrasco-González, C., et al. 2017, *AA*, 607, 74
- Lynden-Bell, D., & Pringle, J. E. 1974, *MNRAS*, 168, 603
- Manara, C. F., Robberto, M., Da Rio, N., et al. 2012, *ApJ*, 755,154
- Manara, C. F., Testi, L., Natta, A., Alcalá, J. M. 2015, *AA*, 579, 66
- Murillo, N. M., Lai, S.-P., Bruderer, S., Harsono, D., & van Dishoeck, E. F. 2013, *A&A*, 560, A103
- Muzerolle, J., Hillenbrand, L., Calvet, N., et al. 2003, *ApJ*, 592, 266
- Najita, J. R., Andrews, S. M., Muzerolle, J. 2015, *MNRAS*, 450, 3559
- Najita, J. R., Strom, S. E., Muzerolle, J. 2007, *MNRAS*, 378, 369
- Najita, J., Carr, J. S., Glassgold, A. E., Shu, F. H., & Tokunaga, A. T. 1996, *ApJ*, 456, 292
- Najita, J. R., Doppmann, G. W., Carr, J. S., Graham, J. R., & Eisner, J. A. 2009, *ApJ*, 691, 738
- Natta, A., Testi, L., & Randich, S. 2006, *AA*, 452, 245 1996, *Nature*, 380, 606
- Ohashi, N., Saigo, K., Aso, Y., et al. 2014, *ApJ*, 796, 131
- Panić, O., Hogerheijde, M. R., Wilner, D., & Qi, C. 2009, *AA*, 501, 269
- Perez, L. M., Carpenter, J. M., Andrews, S. M., et al. 2016, *Science*, 353, 1519
- Piétu, V., Guilloteau, S., & Dutrey, A. 2005, *A&A*, 443, 945
- Piétu, V., Guilloteau, S., Di Folco, E., Dutrey, A., & Boehler, Y. 2014, *AA*, 564, 95
- Schaefer, G. H., Dutrey, A., Guilloteau, S., Simon, M., & White, R. J. 2009, *ApJ*, 701, 698
- Sicilia-Aguilar, A., Henning, T., & Hartmann, L. H. 2010, *ApJ*, 710, 597

- Simon, J. B., Bai, X.-N., Stone, J. M., Armitage, P. J., & Beckwith, K. 2013a, *ApJ*, 764, 66
- Simon, J. B., Bai, X.-N., Armitage, P. J., Stone, J. M., & Beckwith, K. 2013b, *ApJ*, 775, 73
- Simon, J. B., Lesur, G., Kunz, M. W., & Armitage, P. J. 2015, *MNRAS*, 454, 1117
- Simon, M., Dutrey, A., & Guilloteau, S. 2000, *ApJ*, 545, 1034
- Simon, M. N., Pascucci, I., Edwards, S., et al. 2016, *ApJ*, 831, 169
- Siess, L., Dufour, E., & Forestini, M. 2000, *AA*, 358, 593
- Simon, M., Guilloteau, S., Di Folco, E., et al. 2017, *ApJ*, 844, 159
- Takakuwa, S., Saito, M., Lim, J., et al. 2012, *ApJ*, 754, 52
- Takeuchi, T., & Lin, D. N. C. 2002, 581, 1344
- Takeuchi, T., & Lin, D. N. C. 2005, 623, 482
- Tazzari, M., Testi, L., Natta, A., et al. 2017, *A&A*, 606, A88
- Tomida, K., Okuzumi, S., & Machida, M. N. et al. 2016, *ApJ*, 801, 117
- Tripathi, A., Andrews, S. M., Birnstiel, T., & Wilner, D. J. 2017, *ApJ*, 845, 44
- Turner, N. J., Fromang, S., Gammie, C., et al. 2014, in *Protostars and Planets VI*, ed. H. Beuther et al. (Tucson, AZ: Univ. of Arizona Press), 411
- Venuti, L., Bouvier, J., Flaccomio, E., et al. 2014, *AA*, 570, 82
- Yen, H.-W., Koch, P. M., Takakuwa, S., Krasnopolsky, R., Ohashi, N., & Aso, Y. 2017, *ApJ*, 834, 178
- Zhu, Z., Hartmann, L., Gammie, C. F., Book, L. G., Simon, J. B., & Engelhard, E. 2010, *ApJ*, 713, 1134

Table 1. Properties of Class 0 and I Sources

Name	M_* (M_\odot)	\dot{M}_* ($M_\odot \text{ yr}^{-1}$)	R_{gas} (AU)	M_d (M_\odot)	References
TMC-1A	0.64	4(-7)	100	0.04	Aso et al. (2015)
L1551-IRS5	0.5	4(-6)	64		Chou et al. (2014)
HH212	0.2	8(-6)	120		Lee et al. (2014)
L1527	0.3	6(-7)	54		Ohashi et al. (2014)
L1551 NE	0.8	5(-7)	300		Takakuwa et al. (2012)
IRS 63	0.8	1(-7)	170	0.1	Brinch & Jorgensen (2013)
TMC1	0.54	2(-7)	100	0.037	Harsono et al. (2014)
TMR1	0.7		50	0.012	Harsono et al. (2014)
L1536	0.4		80	0.015	Harsono et al. (2014)
Elias 2-27	0.55		300	~0.1	Perez et al. (2016), Tomida et al. (2016)
Lupus 3 MMS	0.3	1(-7)	130		Yen et al. (2017)
L1455 IRS1	0.28	1(-6)	200		Harsono et al. (2014)
VLA 1623	0.2	6(-7)	150		Murillo et al. (2013)

Table 2. Properties of Class II Sources

Name	M_* (M_\odot)	Age (Myr)	R_d (AU)	Ref	R_{CN} (AU)	R_g (AU)	$e(R_g)$ (AU)	Ref, Tracer
AA Tau	0.8	2.0	400	A07	300	≈ 500		K04, CO
AB Aur	2.3	20.9	< 250	890	10	P05, ^{13}CO
BP Tau	0.8	1.7	< 250	...		
CIDA 11	0.4	4.1	< 540	...		
CI Tau	0.8	1.8	233	T17	...	520	13	P14, CN
CW Tau	1.6	2.2	39	P14	< 170	210	7	P14, ^{13}CO
CY Tau	0.4	2.0	66	T17	...	295	11	G14, CN
DE Tau	0.4	0.9	19	P14	< 250	60	20	P14, ^{13}CO
DL Tau	0.8	2.6	175	A07	560	463	6	G14, CO, CN
DM Tau	0.5	5.0	459	T17	610	641	19	G14, CN
DN Tau	0.6	1.3	112	T17	490	241	7	G14, CN
DO Tau	0.5	0.8	44	T17	310	...		
DQ Tau	1.2	3.5	< 210	...		
DR Tau	1.2	1.5	100	A07	< 420	...		
DS Tau	1.0	4.1	70	P14	< 310	180	24	P14, ^{13}CO
FT Tau	0.7	1.6	310	...		
GG Tau	1.3	2.1	490	800		G99, ^{13}CO
GM Aur	1.3	5.6	210	T17	...	525	20	D98, CO
GO Tau	0.6	5.6	336	T17	...	587	55	G14, CN
Haro 6-13	0.6	1.6	441	T17	< 280	> 180		S09, CO
HK Tau	0.5	2.5	320	> 200		J14, CO
HV TauC	0.9	2.7	139	H12	310	256	51	G14, CN
IQ Tau	0.5	1.1	131	T17	560	220	15	G14, CN
LkCa15	1.0	3.7	177	T17	...	567	39	G14, CN
MWC 758	1.7	10.	90	T17	< 450	270	15	C08, CO
RY Tau	2.8	1.0	150	A07	310	≈ 400		C15, CO
SU Aur	2.5	2.9	13	T17	< 140	> 150		P14, ^{13}CO
UZ TauE	0.7	1.3	226	T17	310	300	20	S00, CO
CX Tau	0.4	1.7	12	P14	...	160	20	S17, CO
FM Tau	0.6	3.4	15	P14	...	50	2	S17, CO
IP Tau	0.6	2.8	39	T17	...	95	20	S17, CO
HO Tau	0.6	13.2	62	5	S17, CO
V710 Tau	0.5	1.7	82	6	S17, CO

Note. — A07 (Andrews et al. 2007); C08 (Chapillon et al. 2008); C15 (Coffey et al. 2015); D98 (Dutrey et al. 1998); G99 (Guilloteau et al. 1999); G14 (Guilloteau et al. 2014); H12 (Harris et al. 2012); J14 (Jensen & Akeson 2014); K04 (Kessler-Silacci 2004); P05 (Piétu et al. 2005); P14 (Piétu et al. 2014); S09 (Schaefer et al. 2009); S00 (Simon et al. 2000); S17 (Simon et al. 2017); T17 (Tripathi et al. (2017)